

35. INTERSTITIAL WATER STUDIES ON SMALL CORE SAMPLES, LEG 23 (RED SEA)¹

Frank T. Manheim,² Lee S. Waterman,³ Ching Chang Woo,² and Fred L. Sayles³

ABSTRACT

Sites 225, 277, and 228 in the central and southern-central Red Sea show classical diffusion gradients, approaching saturation in interstitial NaCl with depth as halite beds are approached. Site 228 did not actually encounter halite, but interstitial gradients suggest that it was only several tens of meters deeper than the bottom of the hole. K and Mg were characteristically depleted with depth until the evaporitic layers were approached. Then these constituents and also B and Li increased sharply. At Site 227, intra-halite pore fluids were strongly enriched in Mg (17 g/kg) and Ca (6.7 g/kg), indicating the presence of late stage evaporites, dominated by tachyhydrite, in the salt beds.

The brines associated with evaporite beds resembled the brines in the hot brine metalliferous deeps only in total dissolved solids (about 250 g/kg); chemical composition was notably different. This confirms other evidence that the hot brine deep fluids do not have a local origin but probably rise from deeper layers through fracture channels.

Site 229 showed a relatively small increase in chlorinity (21.5 g/kg at sea floor to 27 g/kg at 210 m). However, considering the extremely rapid rate of accumulation of Quaternary and Pleistocene sediments, this gradient is regarded as sufficient to suggest the presence of salt at depth here also. In contrast, an evaporitic episode in the Red Sea during the Wisconsin glacial maximum, as suggested by Friedman (1972), is not supported by the pore fluid data. Some evaporation and enhancement in salinity in the Red Sea may have occurred, but conditions sufficiently extreme to lay down evaporites in the sea as a whole probably did not occur.

The hot brine deep sediments yielded interstitial fluids roughly comparable with previous analyses both of the hot brines themselves and of associated interstitial waters.

INTRODUCTION

The Red Sea drill holes provided unique opportunities for interstitial water studies. The onboard fluid extractions and determinations of total salinity (by refractometer) soon indicated the presence of salt deposits at depth at Site 225, as well as elsewhere in the Red Sea. It was possible to document, in considerable detail, changes in pore fluid composition approaching and also within rock salt beds, owing to the policy of continuous coring. Since rock salt is virtually impermeable to either fluid flow or ionic diffusion via interconnected porosity, an opportunity was also provided to sample water originally contained in, and between, evaporitic rocks at the time of their burial. Thus, Sites 225, 227, and 228 provide a case study for the

composition of fluids associated with evaporites, leaching and diffusion of dissolved species from buried evaporites, and diagenetic reactions affecting these species on their route upward. The present paper chiefly provides a descriptive survey of the phenomena and does not attempt quantitative assessment of processes occurring in the strata.

Although it was possible to obtain pore fluids from shales even within the highly consolidated evaporitic sequences, the volumes were limited (and continuous coring prevented extensive multiple squeezings). Regrettably, it was not possible to provide fluid for all desirable studies in the deeper portions.

The hot-brine deeps (Site 226, Atlantis II Deep) provided a disappointment, for only shallow and rather disturbed cores were obtained. Hence, it was not possible to obtain pore fluids directly underlying and adjacent to the metalliferous deposits.

In the southern Red Sea Site 229 provided, through its rapid rate of deposition, useful coverage of the Holocene-Pleistocene deposits and conditions in the Red Sea.

¹ Authorized by Director, U.S. Geological Survey.

² U.S. Geological Survey, Woods Hole, Mass.

³ Woods Hole Oceanographic Institution, Woods Hole, Mass. Contribution No. 3195 of the Woods Hole Oceanographic Inst.

METHODS

Shipboard methods have been covered in a separate section (Explanatory Notes, Chapter 2), insofar as they do not repeat standard operations on *Glomar Challenger* (Waterman, 1970). Pore fluids not used immediately for salinity determination (refractometer), field alkalinity measurements, pH, specific gravity, and electrical resistivity were packaged as usual in heat-sealed polyethylene and polypropylene tubes and glass ampules.

Shore laboratory determinations followed previous procedures (Manheim and Sayles, in press) except that most chlorinity determinations (including other halides, bromide, and iodide) were performed with a commercial colorimetric titrator, employing about 0.2 g sample. Cations were analyzed as before by atomic absorption, using seawater (Copenhagen standard) as standards. In view of deviations of the brines from seawater composition, one cannot exclude some systematic errors owing to dissimilarities between samples and standards. The natural deviations of ionic ratios appear to be far larger than probable systematic influences, however. As usual, sodium values by atomic absorption are generally poorer than those obtained by difference between anion species (determined with relatively high precision) and cations (precision 1%–4% with occasional lapses of poorer levels). The “noise” shown in the difference values must be attributed briefly to analytical, rather than real, variations. It is clear, however, that some major shifts in sodium behavior, such as sharply declining NaCl ratios toward the base of Site 227, are due to real effects.

B, Ba, Li, and Sr were determined by direct reading emission spectrometer using high voltage spark excitation and “vacuum cup” electrodes. Beryllium and cadmium served as internal standards.

Special squeezings using a heated squeezer (Manheim, this volume) were performed to assess the influence of rather high presumed temperatures at depth. In the Red Sea, the temperature relationships were reversed from the normal oceanic situation where samples are warmed on being raised to the sea surface and shipboard laboratories. Homogeneity problems, sample manipulations, and analytical scatter may have obscured some of the effects, but shifts in expected directions for K and Mg appear to be present, as noted for samples from Sites 225 and 228 below (Table 1). Temperature effects may be inherent in trace

metal determinations (Presley et al, this volume), but insufficient sample was available to provide analytical materials.

One might also point out that contamination becomes a more serious problem in very consolidated sediments than unconsolidated ones. The contaminant (drilling fluid) may be relatively minor, but it is often more readily or preferentially extracted during squeezing. A few erratic and probably spurious decreases in chloride and other constituents were clearly noted, and these samples were excluded from the tables. Others remain and are noted with parentheses in Figures 3 and 4.

RESULTS

Site 225, Near the Atlantis II Hot Brine Deep

As may be noted in Figure 1 and Table 2, chloride increases gradually and relatively smoothly with depth to about 125 meters. Thereafter, chloride increases sharply down to the halite boundary. K and Mg show gradual depletion with depth until they encounter the evaporitic strata, after which they increase to more than 1.2 and 2.3 g/kg, respectively. Calcium increases to 1.6 g/kg before declining sharply in the evaporite zone. It is evident that K and Mg are being supplied from leaching of evaporites but are evidently depleted by uptake in the sediments a short distance above the Miocene boundary.

A depletion of Sr (Table 3) similar to that of Ca also takes place within the evaporite zone, but boron and lithium increase sharply within it.

Site 226, Atlantis II Deep

The brines extracted from the disturbed sediments in this site resemble the previously described “hot brines” within experimental error, both chemically and isotopically.

Site 227, Near the Atlantis II Hot Brine Deep

Trends similar to those in Site 225 occur down to the evaporite zone, where there are exceptionally sharp increases in Mg concentrations and strong enrichment in Ca, to 17 and 6.6 g/k, respectively. At the same time, strong B, Li, and Sr enrichments are noted. It is clear that these constituents must be supplied by soluble phases within the evaporites, presumably in the form of late stage evaporites.

TABLE 1
Effect of Temperature on Sample Composition

Sample Identification	Subbottom Depth (m)	Description	Na	K	Ca	Mg	Cl
Sta 225 28-1(RT) (24°C)	212	Shale with halite-anhydrite	95.8	1.29	0.69	2.21	(153.3)
Sta 225 28-1(H) (50°C)	212	As above	94.5	1.52	0.68	2.16	153.3
Sta 228 39-1 (55°C)	324	Black-gray shale with brecciated anhydrite	68.4	0.66	1.14	1.32	(110.0)
Sta 228 39-1 (24°C)	324	As above	68.5	0.64	1.25	1.65	110.0

Note: This table shows the difference in composition of samples extracted at laboratory temperature (24°C) from heated (50°C) samples. Values are normalized to constant chlorinity. Samples are from adjacent core materials and may be subjected to variable (slight) amounts of evaporation and contamination. Data from Table 2.

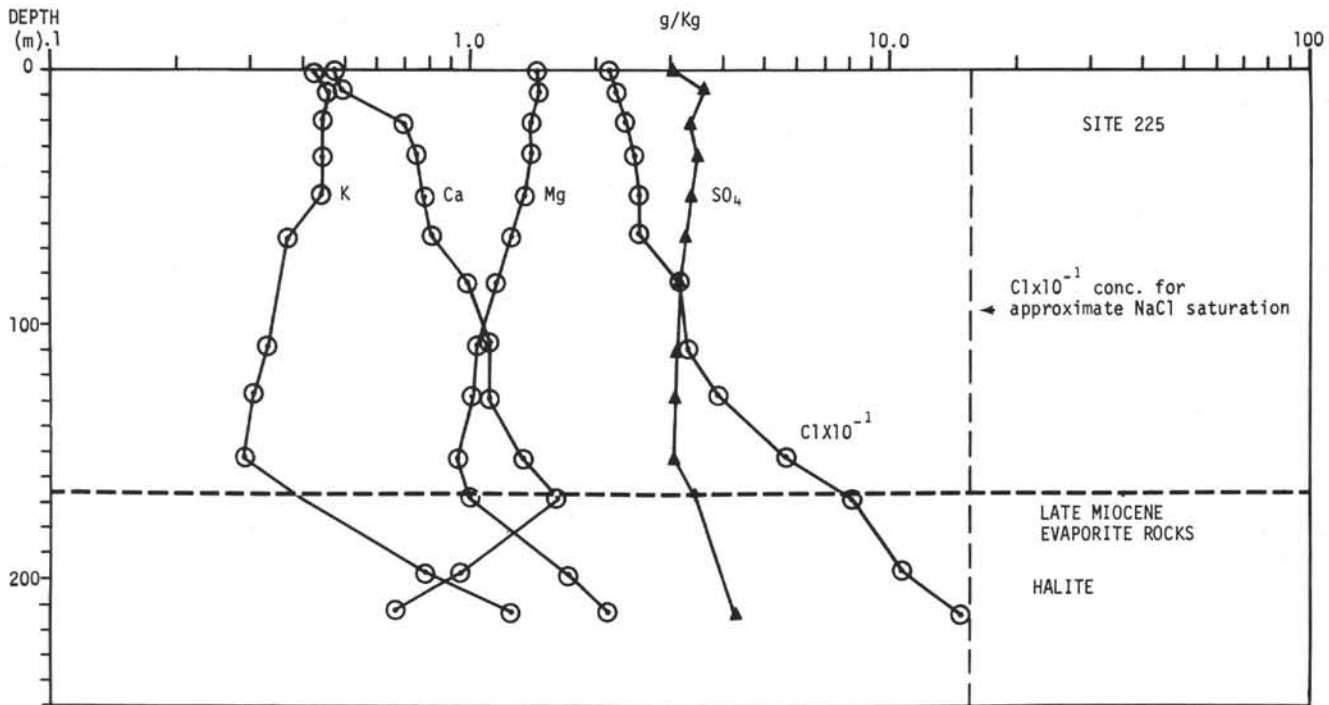


Figure 1. Distribution of major interstitial water components with depth in Site 225.

Although polyhalites were suggested to be present in this section by Stoffers and Kühn (this volume), it is difficult to account for the observed elemental increments by dissolution of polyhalite. Insufficient K and sulfate are present for such a reaction (Table 2 and Figure 2). More suitable from the chemical point of view would be minerals of the bischofite ($\text{MgCl}_2 \cdot 6\text{H}_2\text{O}$)–tachyhydrite ($\text{CaMg}_2\text{Cl}_6 \cdot 12\text{H}_2\text{O}$) type.

Site 228, West Side of Red Sea Axial Valley

Although halite was not penetrated in this site, the increasing interstitial chloride concentrations clearly indicate presence of such beds some tens of meters below penetrated depths (probably less than 100 m). This may be inferred not only from chlorinities, but also from magnesium and potassium upswings (Figure 3). A point of interest is the fact that although the evaporitic strata are intensely brecciated and deformed, overlying strata show relatively little deformation and interstitial gradients are smooth and not interrupted as they would be had faulting or other disruption affected them. At Site 228, pH values are somewhat higher than at other deep sites, and alkalinities may also be somewhat higher; this is associated with relatively depressed calcium values.

Site 229, Southern Red Sea Near Zebayir Island

This site differed from the preceding by losing most of its interstitial sulfate within the first 30 meters of depth. Excess methane with increasing ethane pressures were observed at all depths. Alkalinities, high at first, decreased to low values with depth. One can conclude that methane bacteria were probably a dominant source of the methane gas; these bacteria require absence of significant SO_4 or other oxygen sources and relatively abundant organic matter.

Diagenetic reactions depleting K and Mg and releasing Ca were marked at this site, similar to previous DSDP sites characterized by rapidly accumulated terrigenous sediments having abundant organic matter. The strontium increases to 142 mg/kg also suggest that a significant amount of recrystallization of biogenic calcite or other carbonate species to a lower strontium form has taken place (Manheim et al., 1971).

Site 230, Southern Red Sea

A single core, taken before the drilling vessel was forced to leave the site, nevertheless provided strong evidence that evaporites were present at relatively shallow depth. Chloride increased from a presumed 21.5 g/kg in bottom waters to 33.0 g/kg at a depth estimated at 9 meters. This conclusion is strengthened by the fact that increases in Mg and K were also registered. As one may observe in Figures 1, 2, 3, and 5, Mg and K typically become enriched only within 100 meters or less from evaporite bodies owing to their tendency to be taken up diagenetically in silicate and carbonate minerals.

DISCUSSION

Origin of Brine at Site 227: Dissolution of Late State Evaporite Minerals (Tachyhydrite)

The composition of magnesium and calcium rich brines at the bottom of the section at Site 227 presents a problem and an apparent contradiction to the petrographic observations of Stoffers and Kühn (this volume). These authors report needles of polyhalite toward the base of the section at this site and elsewhere. The problem is that the Ca-rich solutions and absence of significant dissolved SO_4 or K appear to be inherently antithetical to either polyhalite ($\text{K}_2\text{MgCa}_2(\text{SO}_4)_4 \cdot 6\text{H}_2\text{O}$) or appreciable carnal-

lite ($\text{KMgCl}_3 \cdot 6\text{H}_2\text{O}$). In the case of the former, the calcium concentrations should be brought down to lower levels by anhydrite precipitation with sulfate from polyhalite, whereas there is insufficient K to account for more than a small proportion of K-rich species. The proportions of soluble salts that have served as parent materials for the brine at 350 meters at Site 227 may be analyzed as follows:

Chemical Sequence	Na	K	Ca	Mg	Cl	SO ⁴	Total Solids (g/kg)	Total (mol/kg)
1. Starting brine (in mol/kg):	2.95	.023	.168	.690	4.67	.0126	257.6	8.49
2. Removing K as carnallite (There is insufficient sulfate to accommodate all K as polyhalite) leaves:	2.95	—	.168	.667	4.60	.0126	252.0	8.355
3. Removing SO ₄ as anhydrite, leaves:	2.95	—	.155	.667	4.60	—	252.0	8.355
4. Removing Na, as halite, leaves:	—	—	.155	.667	1.65	—	81.5	2.455

Rounding the remainder (above) and placing in mineral form yields $\text{Ca}_{0.6}\text{Mg}_{2.4}\text{Cl}_6 \cdot 12\text{H}_2\text{O}$, a relative of tachyhydrite ($\text{CaMg}_2\text{Cl}_6 \cdot 12\text{H}_2\text{O}$) that is not stable at low temperatures, but would be stable at the probable temperatures occurring at the bottom of Site 227 (Braitsch, 1971).

Expressing the above mineral phases in percentages we have:

Mineral Phase	Weight Percent of Brine Salt	Mol Percent of Brine Salt
Halite NaCl	66.3	69.4
Tachyhydrite $\text{Ca}_{0.6}\text{Mg}_{2.4}\text{Cl}_6 \cdot 12\text{H}_2\text{O}$	31.6	29.0
Carnallite $\text{KMgCl}_3 \cdot 6\text{H}_2\text{O}$	1.5	1.3
Anhydrite CaSO_4	.5	.3

As pointed out by Braitsch (1971), based on previous work by D'ans and by Assarson, systems of tachyhydrite, carnallite, and halite are reasonable, particularly at higher

temperatures. They may be present far more often than is commonly realized because the assemblage is unstable at lower temperatures and extremely hygroscopic, and thus tends to disappear when cores are brought to the surface.

Wisconsin (Glacial Maximum) Evaporitic Sequence in the Red Sea

Friedman (1972) has pointed out that during the Wisconsin glacial maximum the presumed sill depth of the Red Sea at Bab el Mandeb should have caused complete closure of the sea with ensuing evaporite deposition. However, no cores examined by him were found to contain evaporites of any kind. He explained this paradox by postulating consumption of the presumed gypsum by sulfate-reducing bacteria to form sulfides.

Although present deuterium data (Friedman, this volume) show a modest possible increase in interstitial D/H ratio on the upper part of Site 229, no significant interstitial anomaly, either in interstitial chloride nor calcium concentration, was found in the upper 10 meters of the sediments as it should have been to confirm the presumed evaporitic episode. Quantitative calculations to establish the relationships have not yet been made, but a qualitative comparison with the Black and Baltic seas, where anomalous (low) salinities were also created during the glacial maximum, indicates that substantial anomalies should remain after some diffusive smoothing in the post-maximum period. Detailed studies of interstitial salinity on numerous piston cores in the Red Sea (during *Chain Cruise 100* in 1971) likewise showed no indication of intervening maxima in salinity (Milliman, personal communication, based upon unpublished data).

Origin of the Evaporites: Evidence from Interstitial Fluids

A notable feature of the brines is their irregular composition, varying from site to site. Clearly, the brine composition reflects the composition of the more soluble components of underlying evaporites. The isotopic data reported elsewhere in this volume (Lawrence, this volume; Friedman, this volume) show a substantial fresh or meteoric component in the deepest brines and, especially, in brines trapped between salt beds. This variability and fresh water influence is consistent with the concept that the evaporites were laid down in shallow-marine evaporating pans that formed highly variable deposits, depending on local topography, runoff, temperature, and other conditions. Such conditions are also reflected in the petrographic relationships (Stoffers and Kühn, this volume). Deepwater evaporites for the strata penetrated in this study are not favored for they should maintain much heavier isotopic relationships as well as much more consistent (geographic) mineral and brine relationships. Of course, we cannot tell the nature of the environment of the early or median evaporites in the presumably thick deposits from evidence near the top of the section.

One outgrowth of the current study might be the conclusion that highly metastable (at surface conditions) and soluble evaporitic minerals may perhaps be better studied by interstitial water analyses on intervening shales than in the cores themselves unless stringent precautions are taken to prevent dissolution or transformation of the

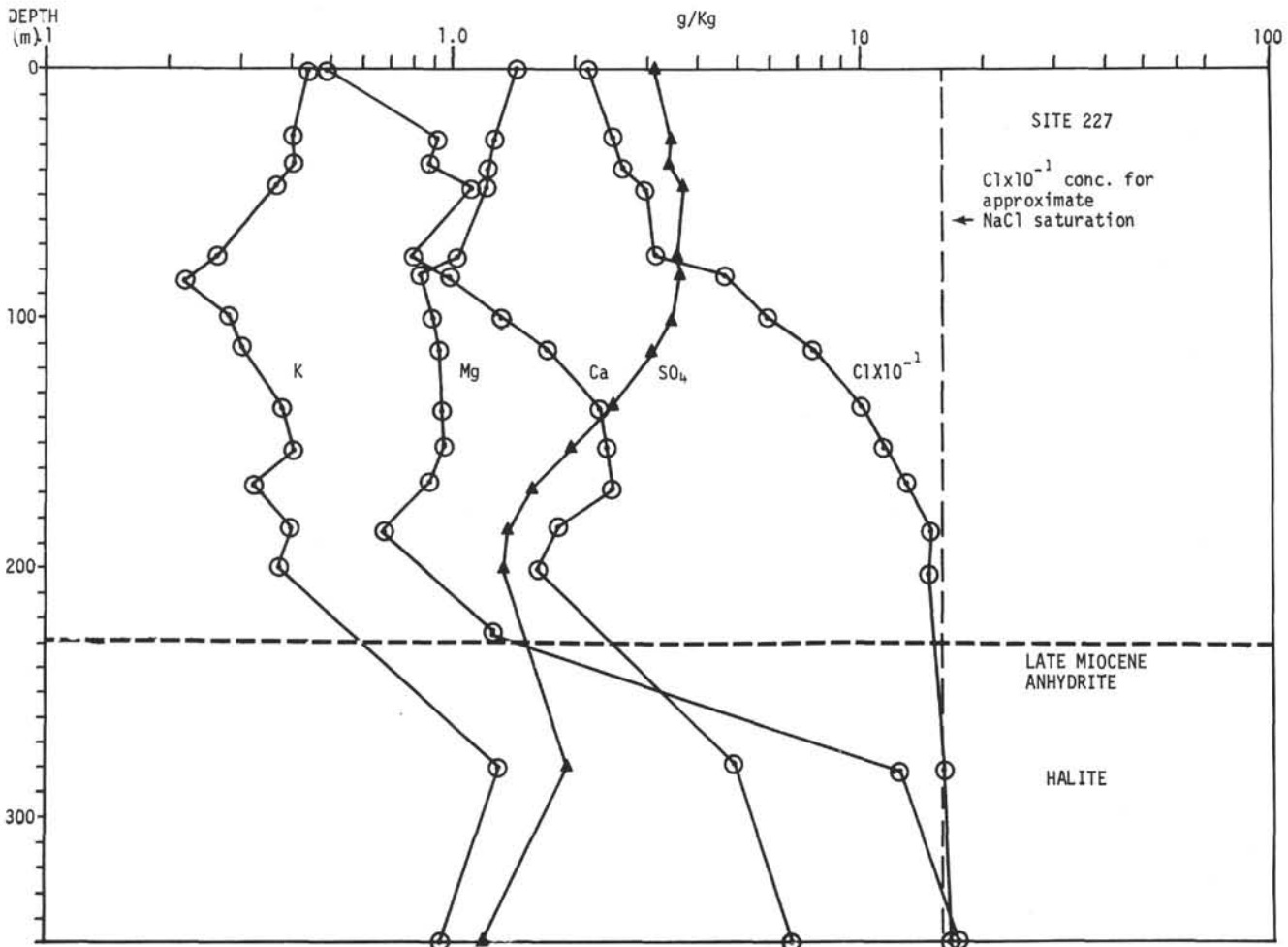


Figure 2. Distribution of major interstitial components with depth in Site 227.

minerals prior to laboratory examination. Diffusion through the shales is a slow process, and extraction of interior uncontaminated pieces can be performed with relatively small change in the brine composition owing to pressure and temperature changes. The temperature changes can also be compensated for in large part. Whereas base exchange (temperature effect) is rapid, mineral precipitation or dissolution within shale beds is generally slow enough so that even metastable solutions can be recovered if extraction is performed immediately.

Relation of the Deep Brines to Fluids from the Atlantis II Deep

The Atlantis II Deep brines are not only substantially different from the three interstitial brines associated with evaporite sites here, but they have maintained substantial constancy in time and place in interstitial waters (see studies in Degens and Ross, 1969). In this respect, the brines appear to come from a large, permeable and communicating reservoir rather than being locally derived, as is presumed for interstitial waters analyzed from Sites 225, 227, and 228. Likewise, the substantial heat suggests migration from deeper horizons. Findings of the diffuser studies, reported elsewhere in the volume, render it highly unlikely for any of the rocks studied here to yield

any sustained flow such as characterizes input into the Atlantis II Deep (Brewer et al., 1971). Thus, the newly analyzed interstitial waters show that, whereas concentrated brines are to be expected at depth throughout the entire evaporite basin of the Red Sea, the brines at the evaporite-normal sediment interface will be variable and are quite different than the hot brines in the metalliferous deeps.

REFERENCES

- Braitsch, O., 1971. Salt deposits, their origin and composition: New York, Heidelberg, (Springer-Verlag), 297 p.
- Brewer, P. G., Wilson, T. R. S., Murray, J. W., Munn, R. G., and Densmore, C. D., 1971. Recent hydrographic observations on the Red Sea brines. A marked temperature increase: *Nature*, 231, p. 37.
- Degens, E. T. and Ross, D. A., 1969. Hot brines and recent heavy metal deposits in the Red Sea: New York, Heidelberg, (Springer-Verlag), 600p.
- Friedman, G. M., 1972. Significance of Red Sea in problem of evaporites and basinal limestones: *Am. Assoc. Petrol. Geol., Bull.* 56, p. 1072.
- Manheim, F. T., Sayles, F. L., and Waterman, L. S., 1971. Interstitial water studies on small core samples, Deep Sea Drilling Project, Leg 8. In Tracey, J. I., Jr., Sutton,

G. H., et al., Initial Reports of the Deep Sea Drilling Project, Volume VIII: Washington (U. S. Government Printing Office), p. 857.

Manheim, F. T. and Sayles, F. L. in press. Composition and origin of interstitial waters of marine sediments, based

on deep sea drill cores. In Goldberg, E. D. (Ed.), The Sea: New York (Interscience), v. 5 (Sillen Memorial).

Waterman, L. S., 1970. Interstitial water program, ship-board manual: Deep Sea Drilling Project, Scripps Inst. of Oceanography, La Jolla. 141 p.

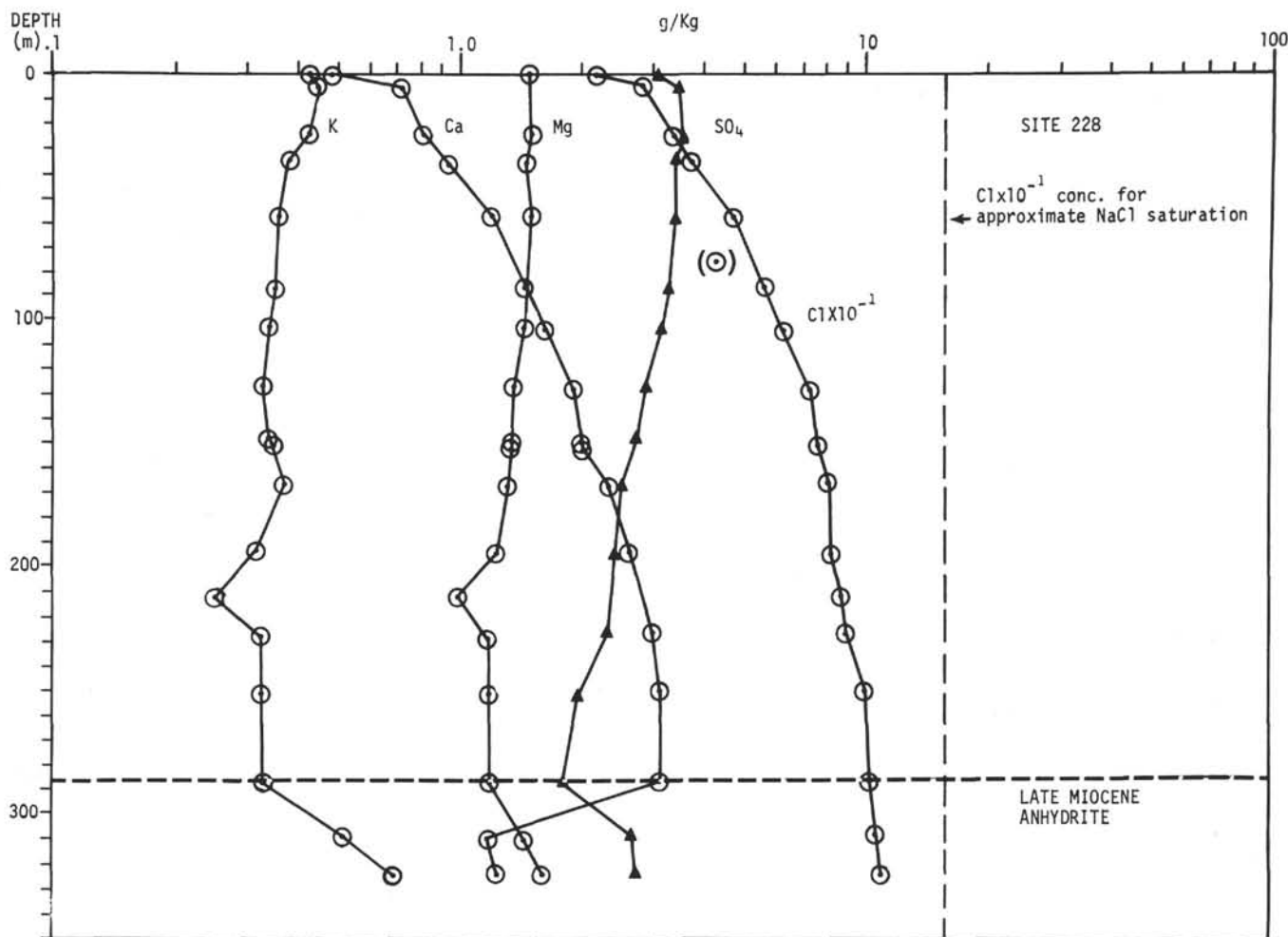


Figure 3. Distribution of major interstitial components with depth in Site 228.

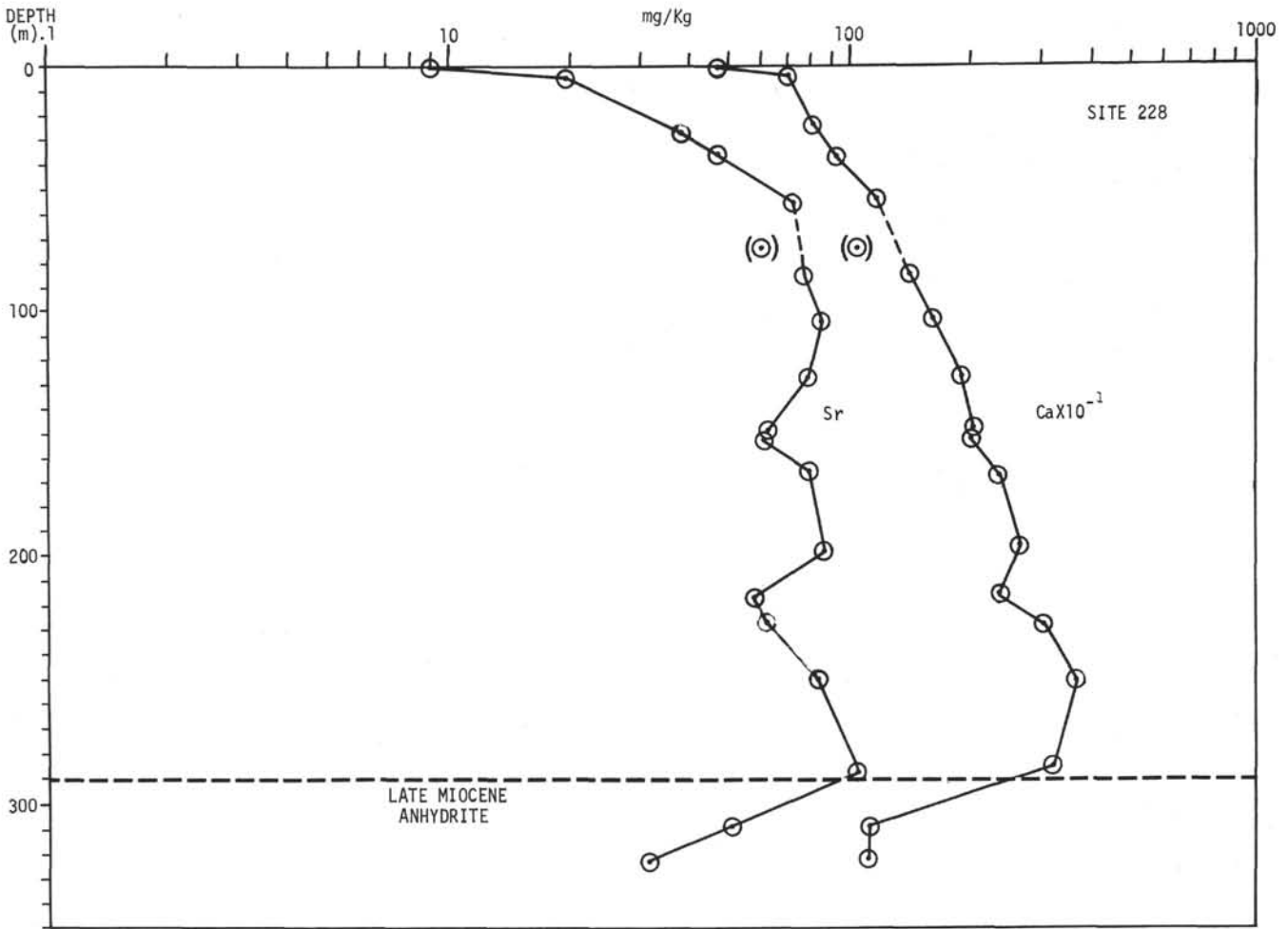


Figure 4. Distribution of interstitial strontium and calcium with depth in Site 228.

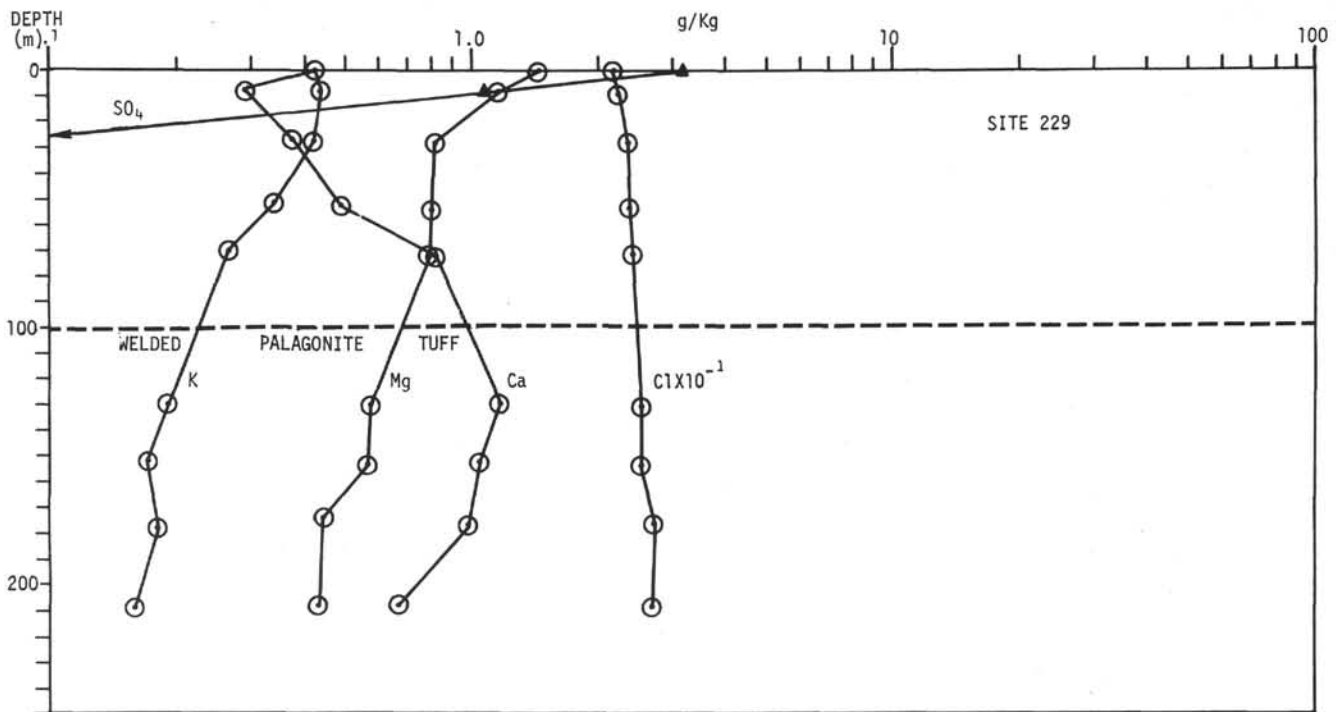


Figure 5. Distribution of major interstitial components with depth in Site 229.

TABLE 2
Major Constituents of Interstitial Waters, Leg 23 (Red Sea)

Sample Core, Section	Subbottom Depth (m)	Age	Description	Na ¹	Na ²	K	Ca	Mg	Total Cations	Cl	SO ₄	Alk	HCO ₃	Total Anions	Sum	Salinity	H ₂ O	pH
Site 225 (21°18.6'N, 38°15.5'E; water depth 1228 m; 16 km E of Atlantic II Deep)																		
<i>Surface ocean water</i>																		
1-5	8	Late Pleistocene	Yellowish-brown detrital clayey silt	12.0	12.1	0.43	0.47	1.42	676	21.5	3.07	(2.4)	(0.14)	612	39.1	39.9		3.5
				12.6	12.5	0.46	0.49	1.47	708	22.5	3.62	1.9	0.12	711	41.2	41.3	35	7.7
3-4	21	Late Pleistocene	Greenish-gray detrital clayey silt mixed with foram-bearing carbonate ooze; highly deformed	13.2	13.2	0.45	0.70	1.40	746	23.8	3.36	4.5	0.28	745	43.2	43.5	26	7.6
5-6	34	Late Pleistocene	Olive-gray detrital silty clay mixed with nanno-rich carbonate ooze; soft, intensely disturbed	13.9	13.9	0.45	0.75	1.41	768	24.6	3.44	2.2	0.13	768	44.7	45.4	41	7.7
8-3	50	Early Pleistocene	Gray detrital clayey silt with foram - bearing carbonate ooze; soupy to soft; intensely disturbed	14.4	14.1	0.44	0.77	1.36	773	25.3	3.37	1.7	0.10	786	45.8	45.4	36	7.9
10-2	64	Late Pliocene	Greenish-gray detrital silty clay with nanno-rich carbonate ooze; soft; intensely deformed	14.4	14.3	0.37	0.82	1.26	775	25.2	3.25	2.3	0.14	781	45.5	45.1	28	7.6
13-6	84	Late Pliocene	Dominantly yellowish-green dolomite bearing detrital silty clay mixed with foram-rich carbonate nanno ooze; disturbed	18.4	(16.6)	0.35	1.01	1.19	(880)	31.5	3.14	2.0	0.12	954	55.7	52.0	25	7.5
16-3	108	Late Pliocene	Olive-gray dolomite bearing detrital clay and nanno ooze; brecciated by drilling	19.4	19.0	0.33	1.11	1.04	975	32.8	3.10	1.4	0.09	993	57.8	53.1	13	7.6
18-4	128	Early Pliocene	Greenish-gray detrital silty claystone interbedded with foram nanno chalk; moderately disturbed	25.5	22.3	0.30	1.10	1.01	1117	39.0	3.08	2.0	0.12	1166	68.0	65.3	25	7.2
21-3	152	Early Pliocene	Gray detrital silty claystone interbedded with dark olive-gray nanno chalk	35.0	34.3	0.29	1.37	0.93	1643	57.0	3.07	2.0	0.12	1674	97.9	35.2	35	7.0
23-2	168	Late Miocene	Dark gray dolomite-rich with detrital silty clay interbedded with black pyrite-rich claystone	50.5	49.9	0.40	1.62	0.99	2343	81.5	3.92			2370	138.4	138.7	15	7.0
26-1	196	Miocene	White anhydrite and black pyrite dolomitic silty claystone	62.6	62.9	0.79	0.95	1.73	2945	104.0		0.6	0.04	2934	170.1	172.0		7.0
28-1(H)	212	Miocene	White halite-anhydrite and nodular anhydrite; shale	94.5	93.0	1.52	0.68	2.16	4335	153.3	(4.3)	1.0	0.06	4419	250.4	242		
28-1(RT)	212	Miocene	White halite-anhydrite and nodular anhydrite; shale	92.7	90.7	1.25	0.67	2.14	4184	148.3	4.22	1.0	0.06	4373	249.4	246		

TABLE 2 – Continued

Sample Core, Section	Subbottom Depth (m)	Age	Description	Na ¹	Na ²	K	Ca	Mg	Total Cations	Cl	SO ₄	Alk	HCO ₃	Total Anions	Sum	Salinity H ₂ O	pH
Site 226 (21°20.5'N, 38°04.9'E; water depth 2169 m; SW part of Atlantis II Deep) ^a																	
1-1	1.5	Holocene	Reddish-black mud; mixture of montmorillonite, anhydrite, and goethite-hematite		94.8	2.07	5.90	0.65			0.95	0.0	0.00			256	6.1
1-2	1.6	Holocene	Reddish-black mud; mixture of montmorillonite, anhydrite, and goethite-hematite	93.8	94.1	2.07	5.91	0.70	4498	158.4	0.72	0.5	0.03	4434	261.6	256	6.0
1-4(IW)	5	Holocene	Reddish-black mud; mixture of montmorillonite, anhydrite and goethite-hematite	92.4	92.8	2.14	6.08	0.69	4452	156.6	0.87	0.1	0.01	4436	238.8		6.4
1-4(H)	5	Holocene	Reddish-black mud; mixture of montmorillonite, anhydrite and goethite-hematite	94.7		1.97	5.61	0.63	4127	158.9	0.97			4502	262.8	244.8	6.4
1-4(HE)	5	Holocene	Reddish-black mud; mixture of montmorillonite, anhydrite and goethite-hematite	94.8	95.1	2.14	5.90	0.67	4541	159.9	0.86			4527	242.9	242.9	6.4
Site 227 (21°19.9'N, 38°08.0'E; water depth 1795 m; eastern flank of Atlantis II Deep)																	
<i>Surface ocean water</i>																	
3-1	27	Late Pliocene	Grayish dolomite-rich carbonate nanno ooze.	11.8 14.7	11.8 14.3	0.43 0.40	0.46 0.93	1.42 1.28	673 784	21.4 24.3	3.06 3.41	1.6 1.6	0.10 0.10	671 758	28.7 45.2	39.3 46.4	6.3 7.5
5-2	38	Late Pliocene	Grayish foram-bearing carbonate nanno chalk	14.7	14.6	0.40	0.88	1.28	793	26.8	3.39	1.4	0.08	799	46.5	46.8	7.2
6-2	46	Late Pliocene	Gray clay-rich chalk interbedded with dark green clay and carbonate rich nanno chalk	17.1	17.0	0.27	1.11	1.21	905	29.4	3.69	1.5	0.09	706	52.9	53.4	7.2
10-2	72	Early Pliocene	Gray carbonate-rich nanno ooze, disturbed by drilling	19.0	18.9	0.26	0.78	1.02	952	31.2	3.47	2.2	0.13	754	55.9	55.2	7.1
12-2	82	Early Pliocene	Greenish-black carbonate and clay-rich nanno chalk interbedded with silt-rich carbonate chalk	28.7	28.1	0.22	0.98	0.84	1354	46.1	3.57	1.5	0.09	1377	80.6	78.6	(7.0)
14-1	100	Early Pliocene	Gray carbonate-rich nanno chalk; homogeneous semilithified	36.4	35.8	0.27	1.31	0.88	1701	58.8	3.36	1.0	0.06	1727	101.1	101.7	7.3
16-1	114	Early Pliocene	Very dark gray nanno-carbonate chalk	47.2	46.1	0.30	1.70	0.92	2173	76.5	3.09	1.5	0.09	2223	129.8	125.0	7.1
18-3	136	Early Pliocene	Gray carbonate-rich nanno chalk	61.3	61.1	0.38	2.32	0.92	2856	99.7	2.43	1.8	0.11	2865	167.2	165.9	6.7
20-3	152	Early Pliocene	Gray silt-rich carbonate-nanno chalk	69.2	69.2	0.40	2.39	0.94	3215	112.7	1.91	1.3	0.08	3219	197.6	187.0	15

TABLE 2 – Continued

Sample Core, Section	Subbottom Depth (m)	Age	Description	Na ¹	Na ²	K	Ca	Mg	Total Cations	Cl	SO ₄	Alk	HCO ₃	Total Anions	Sum	Salinity	H ₂ O	pH	
23-1	167	Early Pliocene	Gray silt-bearing carbonate-nanno chalk	80.2	79.7	0.32	2.44	0.86	3669	129.7	1.55	2.0		3690	215.1	214		6.5	
25-2	186	Early Pliocene	Gray silt-bearing carbonate nanno chalk	93.6	90.6	0.50	1.81	0.67	4100	149.0	1.37			4230	247.0	237	19		
27-1	203	Early Pliocene	Gray dolomite-rich claystone with carbonate and pyrite	91.1	90.4	0.47	1.63	0.87	4098	145.4	1.33			4128	240.8	240	10		
36-2	282	Late Miocene	Anhydrite and dark shale below halite	71.0	70.7	1.29	4.88	12.6	4441	157.1	1.9 ^b			4469	250.7	250.5	23	6.5	
44, CC	350	Late Miocene	Black shale between halite and anhydrite beds	67.4	67.3	0.93	6.67	16.8	4656	164.8	1.2 ^b			4661	257.6	256.0	14	6.2	
Site 228 (19°05.2'N, 38°00.2'E; water depth 1038 m; W side of Red Sea axial valley)																			
1, CC	5	Holocene	Gray foram-nanno-carbonate ooze with detrital clayey silt; soft, homogeneous	16.2	16.4	0.45	0.71	1.50	885	28.5	3.46	1.7	0.10	876	50.9	52.3			
3, CC	26	Late Pleistocene	Gray foram-nanno-carbonate ooze with detrital clayey silt; soupy	19.2	19.0	0.43	0.81	1.47	998	33.1	3.50	1.8	0.11	1007	58.6	58.7	37	7.1	
5-3	36	Late Pleistocene	Greenish-gray foram and carbonate – rich nanno ooze with detrital sandy silt	22.1	21.7	0.38	0.94	1.45	1122	37.7	3.36	2.2	0.13	1136	66.0	65.5	24	7.3	
7-6	58	Late Pleistocene	Gray-olive-green carbonate ooze and detrital clayey silt	28.3	27.9	0.36	1.20	1.50	1405	47.9	3.38	2.3	0.14	1424	82.8	81.9	22	7.1	
10-6	76	Late Pleistocene	Greenish-gray and greenish-black detrital clayey silt and silty clay	25.4	25.0	0.35	1.04	1.45	1266	42.9	3.22	2.1	0.13	1280	74.5	74.3	23	7.1	
11-4	87	Late Pleistocene	Olive-gray detrital silty clay-rich carbonate ooze	34.1	33.4	0.35	1.44	1.46	1656	57.2	3.26	2.1	0.13	1684	99.9	97.4	21		
13, CC	105	Late Pleistocene	Green detrital sand-silt-clay; rich in forams	37.8	38.3	0.34	1.61	1.44	1873	63.4	3.15	1.8	0.11	1854	107.8	110.7	17	6.9	
16-5	129	Late Pleistocene	Gray detrital clayey silt and carbonate chalk	43.9	43.6	0.33	1.91	1.37	2112	73.2	2.91	1.4	0.08	2126	123.8	122.8		6.9	
18-2	150	Late Pleistocene	Olive carbonate-detrital clayey siltstone	46.2	45.3	0.34	2.01	1.35	2189	77.0	2.79	0.5	0.03	2229	129.7	129.7	15	7.1	
19-2	153	Late Pleistocene	Gray carbonate-detrital clayey siltstone and detrital clayey silt-rich carbonate chalk	45.2	45.8	0.35	2.00	1.36	2212	75.5	2.67			2186	127.1	129.0	19		
21-2	167	Late Pliocene	Grayish-olive detrital clayey silt-carbonate chalk	49.3	49.0	0.37	2.35	1.34	2368	81.6	2.50	1.0	0.06	2355	137.5	136.7	16	6.6	
24-3	196	Late Pliocene	Greenish-gray alternating beds of claystone, chalk and siltstone	48.2	52.5	0.32	2.65	1.24	2553	81.9	2.43	0.9	0.05	2369	136.9	147.0	14	6.3	

TABLE 2 – Continued

Sample Core, Section	Subbottom Depth (m)	Age	Description	Na ¹	Na ²	K	Ca	Mg	Total Cations	Cl	SO ₄	Alk	HCO ₃	Total Anions	Sum	Salinity	H ₂ O	pH
26-3	214	Late Pliocene	Greenish-gray carbonate-detrital clayey siltstone	53.9		0.25	2.33	0.99		88.7	2.34	0.7	0.04	2550	148.5	159.0	25	6.3
28-2	228	Late Pliocene	Greenish-gray to olive-gray foram-bearing carbonate-detrital siltstone	54.2	55.4	0.33	2.99	1.20	2664	90.9	2.31	0.8	0.05	2612	152.0	153.5	16	
30-4	251	Late Pliocene	Greenish-gray carbonate detrital siltstone	59.9	60.7	0.30	3.69	1.20	2931	101.2	1.99	1.7	0.10	2396	168.4	170.0	11	
35-1	288	Late Miocene	White anhydrite and gray-black siltstone	62.0	61.6	0.33	3.13	1.20	2942	103.6	1.80	1.6	0.10	2960	172.1	170.0		7.5
37-1	310	Late Miocene	Brecciated anhydrite interbedded with black to gray siltstone	66.7	66.0	0.52	1.20	1.46	3062	107.5	2.75	1.4	0.08	3092	180.2	178.8		7.0
39-1	324	Late Miocene	Brecciated anhydrite interbedded with black shale	68.5 ^c	(84.7)	0.64	1.25	1.65	3899	110.0	(2.7)			3103	184.7	(210.0)		
39-1(H)	324	Late Miocene	Brecciated anhydrite interbedded with black-gray shale	72.0	69.1	0.70	1.20	1.39	3197	115.7	2.76			3322	193.8	(190.3)		
Site 229 (14°46.1'N, 42°11.5'E; water depth 852 m; shallow basin S of Zebayir Island)																		
1, CC	9	Holocene	Olive-gray clay-bearing nanno carbonate ooze	12.5	12.8	0.49	0.29	1.14	675	22.4	1.08	9.3	0.56	663	38.3	392.0		7.4
2A-1	29	Holocene	Light olive clay and nanno-rich carbonate ooze	13.4	13.6	0.41	0.38	0.81	689	23.7	0.06	6.8	0.41	670	39.0	40.2	34	7.4
2-6	54	Upper Pleistocene	Olive-gray clay-rich nanno carbonate ooze	13.2	13.8	0.34	0.49	0.81	701	23.6	0.02	4.9	0.30	670	38.9	40.6	34	7.5
5A-6	72	Upper Pleistocene	Dusky yellow-green glass-bearing clay and nanno-rich carbonate ooze	13.1	13.5	0.26	0.82	0.79	697	24.1	0.01	2.7	0.16	682	39.2	40.8	29	(7.0)
9A-2	131	Upper Pleistocene	Pale olive silty clay and carbonate-rich nanno ooze	14.1	13.9	0.19	1.15	0.57	715	25.4	0.01			717	41.4	42.1	43	7.3
12A-4	155	Upper Pleistocene	Pale olive foram-bearing silty clay and carbonate-rich nanno ooze and chalk	14.0	14.1	0.17	1.04	0.57	717	25.0	0.10	1.6	1.0	711	41.0	42.0	33	6.9
18A-5	210	Upper Pleistocene	Pale olive silty clay and carbonate-rich nanno chalk	15.9	15.5	0.16	0.67	0.43	747	26.9	0.10	2.0	0.1	763	44.2	(43.3)	(52 ^d)	
Site 230 (15°19.0'N, 41°50.0'E, water depth 832 m, W side of axial valley W of Zebayir)																		
1, CC	9	Holocene	Yellowish-green to pale olive carbonate nanno ooze; contains pteropods, foram, and zeolite	17.2	18.7	0.58	0.73	1.65	999	33.0		3.3	0.20	935	53.3	59.0		7.4

Note: All values in g/kg except for alkalinity (meg/kg), total water (H₂O) in %, and pH. Na¹ refers to values calculated by difference; Na² indicates direct determination by atomic absorption. HCO₃ is calculated on assumption that total alkalinity is attributable to HCO₃ ion. Cl refers to total halogens. Sum indicates calculated Na, whereas total cations include directly determined value. Salinity refers to refractive index determination (generally shipboard). Where two Alkalinity values are given, uppermost refers to shipboard determination; lower one laboratory.

^aSamples from Site 226 are subject to especially large uncertainty owing to disturbance of core (contamination with bottom water) and possible evaporative effects of hot fluid sample before and during sampling.

^bEstimated from remaining data at in situ temperature by B. F. Jones, USGS Washington, using WATEQ computer program to calculate chemical equilibria in natural water (Nat'l Tech Inf Service PB-220464: A. H. Truesdell and B. F. Jones, 1973). Solubility of anhydrite provides constraining condition.

^cDetermined from Na/Cl ratio.

^dSample taken for fluid extraction did not corroborate this high water content; probably erroneous.

TABLE 3
Minor Constituents (in mg/kg), Leg 23 (Red Sea)

Sample Core, Section	Subbottom Depth (m)	Age	B	Ba	Li	Sr	Sample Core, Section	Subbottom Depth (m)	Age	B	Ba	Li	Sr
Site 225 (21°18.6'N, 38°15'E; water depth 1228m; 16 km E of Atlantis II Deep)							Site 228 (19°05.2'N, 39°00.2'E; water depth 1038 m; W side of Red Sea axial valley)						
Surface ocean water			5.5	<0.1	0.2	8.8	1-3	5	Holocene	5.0	<0.1	0.5	20.0
1-6	8	Late Pleistocene	5.5	<0.1	0.4	9.6	3, CC	26	Late Pleistocene	5.5	<0.1	0.2	38.0
3-4	21	Late Pleistocene	5.0	0.4	0.1	10.5	5-3	36	Late Pleistocene	6.0	—	0.2	47.0
5-6	34	Late Pleistocene	7.0	0.2	0.3	29.0	7-6	58	Late Pleistocene	6.0	0.1	0.3	72.0
8-3	50	Early Pleistocene	5.5	0.2	0.4	32.0	10-6	76	Late Pleistocene	6.0	0.2	0.4	59.0
10-2	64	Late Pliocene	4.0	0.2	0.7	33.0	11-4	87	Late Pleistocene	5.0	<0.1	0.4	67.0
13-6	84	Late Pliocene	4.5	<0.1	0.2	30.0	13, CC	105	Late Pleistocene	6.5	<0.1	0.6	84.0
16-3	108	Late Pliocene	5.5	0.8	0.9	42.0	16-5	129	Late Pleistocene	5.5	—	0.7	78.0
18-4	128	Early Pliocene	6.5	0.4	1.0	49.0	18-2	150	Late Pleistocene	<4.0	0.7	0.7	62.0
21-3	152	Early Pliocene	9.0	0.4	1.4	57.0	19-2	153	Late Pleistocene	4.0	0.4	0.6	60.0
23-2	168	Late Miocene	5.0	<0.16	1.1	27.0	21-2	167	Late Pliocene	6.0	0.5	1.0	79.0
26-1	196	Miocene	5.5	<0.18	1.5	11.5	24-3	196	Late Pliocene	6.0	<0.1	1.3	87.0
28-1 (H)	212	Miocene	—	—	—	—	26-3	214	Late Pliocene	4.5	0.2	0.8	56.0
Site 226 (21°20.5'N, 38°04.9'E; water depth 2169 m; SW part of Atlantis II Deep)							Site 229 (14°46.1'N, 42°11.5'E; water depth 852 m; shallow basin S of Zebayir Island)						
1-1	1.5	Holocene	10.0	1.0	4.7	46.0	1, CC	1	Holocene	6.0	<0.1	0.2	10.2
1-2	1.6	Holocene	9.5	0.9	5.1	43.0	2A-1	29	Holocene	7.0	0.5	0.2	23.0
1-4 (1W)	5	Holocene	9.0	1.1	5.3	46.0	2-6	54	Upper Pleistocene	7.5	0.4	0.2	40.0
1-4 (H)	5	Holocene	8.0	1.4	7.5	32.0	5A-6	72	Upper Pleistocene	4.5	0.6	0.1	69.0
1-4 (He)	5	Holocene	15.0	2.6	6.8	72.0	3-5	99	Upper Pleistocene	6.5	0.1	0.4	85.0
Site 227 (21°19.9'N, 38°08.0'E; water depth 1795 m; eastern flank of Atlantis II Deep)							Site 230 (15°19.0'N, 41°50.0'E; water depth 832 m; W side of axial valley W of Zebayir Island)						
Surface ocean water			5.0	—	0.2	8.8	9A-2	131	Upper Pleistocene	6.0	0.5	0.2	137.0
		Late Pliocene	9.3	<0.1	0.4	19.2	12A-4	155	Upper Pleistocene	5.5	0.3	0.2	137.0
		Late Pliocene	5.0	0.1	0.7	21.8	15A-1	177	Upper Pleistocene	8.0	1.5	0.4	142.0
		Late Pliocene	4.0	0.4	0.2	18.2	18A-5	210	Upper Pleistocene	8.0	1.0	0.4	109.0
10-2	75	Early Pliocene	5.0	<0.1	0.6	26.0	Site 230 (15°19.0'N, 41°50.0'E; water depth 832 m; W side of axial valley W of Zebayir Island)						
12-2	82	Early Pliocene	4.5	<0.1	0.9	27.0	1, CC	9	Holocene	8.5	<0.1	0.2	44.0
14-1	100	Early Pliocene	7.0	0.2	(2)	42.0							
16-1	144	Early Pliocene	4.0	<0.1	1.0	28.0							
18-3	136	Early Pliocene	8.0	0.1	2.1	46.0							
20-3	152	Early Pliocene	8.5	0.1	3.2	72.0							
23-1	167	Early Pliocene	5.5	0.1	1.7	34.0							
25-2	186	Early Pliocene	<4.0	0.1	<0.1	4.6							
27-1	203	Early Pliocene	<4.0	1.3	1.7	20.0							
30-1	228	Early Pliocene	—	—	—	—							
36-2	282	Late Miocene	74.0	0.1	13.3	99.0							
44, CC	350	Late Miocene	—	—	—	—							

ACKNOWLEDGMENTS

We wish to especially thank the shipboard technicians of Leg 23 for efficiently and conscientiously assisting in collecting and documenting the large fund of data on which this report is based. These technicians, led by R. J. Iuliucci, were K. Van Allyn, B. W. Hamlin, M. L. Henry, G. L. Jones, D. F. Marsie, L. G. Russill, L. G. Schneider, D. Siems and P. G. Thompson. We thank Captain J. Clarke and his crew in particular for their efforts in manually keeping *Glomar Challenger* on station when the computer could not cope

and T. Bangs for his advice and guidance on how to reach our scientific objectives. The geochemical program in the Red Sea was especially successful due to the preparations and enthusiasm of F. T. Manheim. Many people assisted us in choosing sites by freely allowing access to unpublished data and by discussions. We are indebted, therefore, to H. Backer; E. T. Bunce; J. I. Ewing; M. Ewing; R. Harbison; J. I. Heirtzler; J. M. Hunt; A. S. Laughton; D. H. Matthews; G. Pyre, and his colleagues of the Gulf Oil Company, London; F. Sayles; and M. Talwani. The assistance of the Deep Sea Drilling Project staff in all the phases of Leg 23 is gratefully acknowledged.